Discrete versus Continuous Wires on Quantum Networks

ARTICLE *in* THE JOURNAL OF PHYSICAL CHEMISTRY B · APRIL 2009

Impact Factor: 3.3 · DOI: 10.1021/jp8065986 · Source: PubMed

2 AUTHORS:

Amnon Aharony
Ben-Gurion University of the Negev
280 PUBLICATIONS **10,904** CITATIONS
SEE PROFILE

O. Entin-Wohlman
Tel Aviv University
291 PUBLICATIONS **5,592** CITATIONS
SEE PROFILE

Discrete versus continuous wires on quantum networks

Amnon Aharony* and Ora Entin-Wohlman*
Department of Physics and the Ilse Katz Center for Meso- and Nano-Scale Science and Technology, Ben Gurion University, Beer Sheva 84105, ISRAEL

(Dated: July 25, 2008)

Mesoscopic systems and large molecules are often modeled by graphs of one-dimensional wires, connected at vertices. In this paper we discuss the solutions of the Schrödinger equation on such graphs, which have been named "quantum networks". Such solutions are needed for finding the energy spectrum of single electrons on such finite systems or for finding the transmission of electrons between leads which connect such systems to reservoirs. Specifically, we compare two common approaches. In the "continuum" approach, one solves the one-dimensional Schrödinger equation on each continuous wire, and then uses the Neumann-Kirchoff-de Gennes matching conditions at the vertices. Alternatively, one replaces each wire by a finite number of "atoms", and then uses the tight binding model for the solution. Here we show that these approaches cannot generally give the same results, except for special energies. Even in the limit of vanishing lattice constant, the two approaches coincide only if the tight binding parameters obey very special relations. The different consequences of the two approaches are demonstrated via the example of a T-shaped scatterer.

I. Introduction

The quantum mechanics of electrons on networks, made of one-dimensional (1D) wires which are connected at vertices, has been the subject of active research for a long time. This research probably started with the study of organic molecules, in 1953.[1,2] However, it gained a large momentum in 1981, when P. G. de Gennes considered the linearized Landau-Ginzburg equations on networks, in connection with percolating superconductors.[3,4] This work was later extended by Alexander.[5] In the last 25 years, quantum networks have been used as theoretical models of mesoscopic systems, which have become experimentally available due to the advancements in microfabrication. In these models, the 1D wires represent limits of three dimensional wave guides, which are assumed to be sufficiently narrow to justify keeping only the lowest transverse mode. Quantum networks are also used to model novel molecular devices, where each wire consists of discrete atoms.

In this paper we compare several approaches for solving the single electron Schrödinger equation on such networks. Basically, this solution consists of two stages. First, one solves the equation on each wire. Denoting the vertices at the ends of the wire by α and β, one can express the solution inside the wire, $\psi_{\alpha\beta}(x_{\alpha\beta})$ (where $x_{\alpha\beta}=0$ at vertex α and $x_{\alpha\beta}=L_{\alpha\beta}$ at vertex β) in terms of the wave functions at its ends, Ψ_α and Ψ_β. At the next stage, one must employ some matching conditions at each vertex. Using these matching conditions, and eliminating the wave functions inside each wire, one ends up with a set of discrete linear equations for the wave functions at the vertices,

$$M_{\alpha\alpha}\Psi_\alpha+\sum_\beta M_{\alpha\beta}\Psi_\beta=0, \tag{1}$$

where the coefficients $M_{\alpha\beta}$ are determined by the 1D solution on each wire and by the matching conditions. Obviously, the detailed solution for the network depends on the latter.

There have been several approaches to the issue of the matching conditions. Some of the earlier papers in mesoscopics used the scattering approach.[6,7,8] For a vertex with $\mathcal{N}_\alpha$ wires, this approach constructs an $\mathcal{N}_\alpha\times\mathcal{N}_\alpha$ unitary scattering matrix,[9] which relates the amplitudes of the $\mathcal{N}_\alpha$ incoming (plane) waves to the $\mathcal{N}_\alpha$ outgoing waves. Given this matrix, one can solve for the amplitudes of the two waves in each wire, and thus find a full solution for the wave functions on the network. For the examples treated in these early papers, the scattering matrix was parametrized arbitrarily. To find explicit values for the elements of the scattering matrix, one must solve a more "microscopic" model, as done e.g. in Refs. 10 and 11.

A widely used second approach follows de Gennes,[3,4] and uses the so called Kirchoff (or Neumann) matching condition at the vertices.[12,13,14,15,16,17,18] Given the continuous solutions $\psi_{\alpha\beta}(x_{\alpha\beta})$ on each of the $\mathcal{N}_\alpha$ wires which meet at vertex α, one requires continuity of the wave function, $\psi_{\alpha\beta}(0)\equiv\Psi_\alpha$, and also the condition

$$\sum_{\beta=1}^{\mathcal{N}_\alpha}\frac{\partial\psi_{\alpha\beta}}{\partial x_{\alpha\beta}}\Big|_{x_{\alpha\beta}=0}=0, \tag{2}$$

where the sum is over the $\mathcal{N}_\alpha$ wires which meet at vertex α. Since the outgoing probability current on wire $(\alpha\beta)$ is proportional to

$$I_{\alpha\beta}=\Im[(\psi_{\alpha\beta})^*(\partial\psi_{\alpha\beta}/\partial x_{\alpha\beta})], \tag{3}$$

Eq. (2) supplies a sufficient condition for the conservation of the probability at this vertex.

However, Eq. (2) does not represent a *necessary* condition for the conservation of current. A more general condition is given by

$$\sum_\beta\frac{\partial\psi_{\alpha\beta}}{\partial x_{\alpha\beta}}\Big|_{x_{\alpha\beta}=0}=\lambda_\alpha\Psi_\alpha, \tag{4}$$

with any real λ_α.[19,20,21,22] Multiplying both sides of this equation by $(\Psi_\alpha)^*$ yields a real number, which does not contribute to the current in Eq. (3). For a vertex with two wires, λ_α represents the strength of a delta-function potential at the vertex.[22] An infinite value of λ_α in Eq. (4) implies that $\Psi_\alpha = 0$, which is known as the Dirichlet matching condition. In this limit, there is no probability current through this vertex. Thus, finite values of λ_α interpolate between the Neumann and the Dirichlet limits. However, for real networks one still needs to derive λ_α from some microscopic equations.

An alternative approach, which avoids some of these ambiguities, is based on the *tight binding model*, as done e.g. in Ref. 10. In this approach, the system is described by a set of localized wave functions, associated with discrete "atomic" sites $\{n\}$. This approach is often used for molecules, where it is equivalent to the method of linear combination of atomic orbitals (LCAO). It is also used for the calculation of energy bands in periodic lattices.[23] The discrete Schrödinger equations for the amplitudes $\{\psi_n\}$ of the "atomic" stationary wave functions for an energy ϵ are then given by

$$(\epsilon - \epsilon_n)\psi_n = -\sum_m J_{nm}\psi_m. \qquad (5)$$

Here, ϵ_n and $-J_{nm}$ are the diagonal and the off-diagonal matrix elements of the Hamiltonian, in the basis of the atomic wave functions. For real molecules or crystals, these matrix elements can be calculated from the atomic wave functions and from the microscopic potentials seen by the electron.[23] The tight binding equations have also been applied to a variety of specific mesoscopic quantum networks, where the "atoms" represent quantum dots; see e. g. Refs. 10, 24,25,26,27 and references therein.

For 1D chains, the results of the discrete tight-binding model approach those of the continuous Schrödinger equation when one sends the lattice constant of the former to zero (see below). However, in this paper we show that generally this limit is problematic for more complex networks. Section II presents the derivation of Eq. (1) for continuous wires and for discrete wires (described by the tight binding Hamiltonian), and contains a critical comparison between them. Section III demonstrates the difference between the two approaches for the simplest example of a T-shaped scatterer, and Sec. IV contains our conclusions.

II. The equations for the vertex wave functions

As stated above, applying the Neumann matching conditions to the wave functions describing the continuous wires yields Eq. (1). Here we first rederive this equation for the more general matching condition (4), then derive a similar equation from the solution of the discrete model, and finally compare the two resulting equations.

A. Continuous graphs

For simplicity, we follow much of the literature and assume that there is no potential energy within the wires. We start by solving the continuous 1D Schrödinger equation for a free particle on each 1D wire. For a given energy, ϵ, the solutions are linear combinations of e^{ikx} and e^{-ikx}, with $\epsilon = \hbar^2k^2/(2m)$. Here we used the simplifying assumption that the effective mass m is the same on all the wires (in general one could have a different wave vector k for each wire, for the same energy ϵ). We next express the solution $\psi_{\alpha\beta}$ on the wire $(\alpha\beta)$ in terms of the wave functions at its two ends,[16,19] which we denote by Ψ_α and Ψ_β:

$$\psi_{\alpha\beta}(x_{\alpha\beta}) = \Psi_\alpha \frac{\sin[k(L_{\alpha\beta} - x_{\alpha\beta})]}{\sin(kL_{\alpha\beta})} + \Psi_\beta \frac{\sin(kx_{\alpha\beta})}{\sin(kL_{\alpha\beta})}. \quad (6)$$

Substituting these expressions into the matching condition (4) then yields

$$\sum_\beta k\left[-\Psi_\alpha \cot(kL_{\alpha\beta}) + \Psi_\beta/\sin(kL_{\alpha\beta})\right] = \lambda_\alpha \Psi_\alpha. \quad (7)$$

Generally k could have different values for different wires. Assuming the same k for all wires, this can be rewritten in the form of Eq. (1), with

$$M_{\alpha\alpha} = \frac{\lambda_\alpha}{k} + \sum_\beta \cot(kL_{\alpha\beta}), \quad M_{\alpha\beta} = -\frac{1}{\sin(kL_{\alpha\beta})}. \quad (8)$$

Indeed, $\lambda_\alpha \to \infty$ implies that $M_{\alpha\alpha} \to \infty$, and therefore $\Psi_\alpha = 0$, as in the Dirichlet limit. The solution of the set of linear equations (1) then either yields ratios among the Ψ's at a given energy ϵ (for a scattering problem) or gives the set of spectrum of allowed ϵ's (for an eigenvalue problem).

B. The tight binding model

We now replace the $(\alpha\beta)$ wire by a discrete chain of "atoms". For simplicity, we assume that all the wires have the same lattice constant a. The wire $(\alpha\beta)$ now has $N_{\alpha\beta} + 1$ "atoms", at sites $x_{\alpha\beta} = na$, where $n = 0, 1, 2, ..., N_{\alpha\beta}$. The length of the wire is then given by $L_{\alpha\beta} = aN_{\alpha\beta}$. Assuming no potential energy within each wire also allows us to set the diagonal site energies ϵ_n within each wire equal to zero. For simplicity we also assume uniform nearest-neighbor "hopping" matrix elements, $J_{n,n\pm1} = J$. For $0 < n < N_{\alpha\beta}$, the tight binding equation (5) becomes

$$\epsilon\psi_{\alpha\beta}(n) = -J[\psi_{\alpha\beta}(n-1) + \psi_{\alpha\beta}(n+1)], \qquad (9)$$

with solutions e^{ikna} or e^{-ikna} and with the dispersion relation

$$\epsilon = -2J\cos(ka). \qquad (10)$$

(Again, if different wires have different J's or different a's then each wire will have its own k, for the same ϵ).

Fixing the wave functions at the ends of the wire, $\psi_{\alpha\beta}(0) = \Psi_\alpha$ and $\psi_{\alpha\beta}(N_{\alpha\beta}) = \Psi_\beta$, the solution along the chain $(\alpha\beta)$ becomes

$$\psi_{\alpha\beta}(n) = \frac{\sin[ka(N_{\alpha\beta} - n)]}{\sin(kaN_{\alpha\beta})}\Psi_\alpha + \frac{\sin(kan)}{\sin(kaN_{\alpha\beta})}\Psi_\beta. \quad (11)$$

As might be expected, this solution is just a discrete version of Eq. (6), but with the modified dispersion relation (10).

We next write down the tight binding equation (5) for the vertex site α, where we do allow for a non-zero site energy ϵ_α:

$$(\epsilon - \epsilon_\alpha)\Psi_\alpha = -J\sum_\beta \psi_{\alpha\beta}(n = 1). \quad (12)$$

Substituting Eq. (11), and using Eq. (10) (with the same k on all wires), this again yields Eq. (1), and $M_{\alpha\beta}$ is again given by Eq. (8). However, the diagonal coefficient is different:

$$M_{\alpha\alpha} = \sum_\beta [\cot(kaN_{\alpha\beta}) - \cot(ka)] + 2\cot(ka) + \epsilon_\alpha/[J\sin(ka)]. \quad (13)$$

Note that in some sense Eq. (1) has the same form as the discrete Schrödinger equation (5) for the vertices of the network. However, unlike the J_{nm}'s and ϵ_n's of that equation, the coefficients $M_{\alpha\alpha}$ and $M_{\alpha\beta}$ do depend on the energy ϵ which characterizes the solution. Note also that these renormalized coefficients reduce back to those in Eq. (5) when all the wires reduce to single bonds, $N_{\alpha\beta} = 1$.

C. Comparison

Comparing Eq. (13) with Eq. (8), we see that the two equations would become identical only when

$$\lambda_\alpha/k = \epsilon_\alpha/[J\sin(ka)] - (\mathcal{N}_\alpha - 2)\cot(ka). \quad (14)$$

(Again: the terms which depend on ka should be replaced by sums of such terms with different k's if the wires have different parameters). The on-site energy on the vertex ϵ_α represents a diagonal matrix element of the Hamiltonian, and therefore it should not depend on the energy ϵ which represents the specific solution for the Schrödinger equation. Therefore, Eq. (14) implies that the "equivalent" continuum Hamiltonian would have parameters λ_α which generally depend on ϵ. However, the λ_α's represent the matching conditions, and these are also characteristic of the system and not of its solutions. Therefore, in general one cannot choose energy-independent vertex parameters for which the two approaches yield the same solutions everywhere.

Interestingly, the difference between the two approaches is largest when $\cot(ka)$ is large, namely near the band edges. Usually, divergences near the 1D band edges are associated with van Hove singularities, which cause the divergence of the density of states. For this reason, the use of tight binding equations is often restricted to the vicinity of the band center, i. e. $ka \sim \pi/2$. However, even in this region the two models become identical only *at* the band center $\epsilon = 0$ and not at any other energy. Furthermore, although one can choose the electron energy (i. e. the Fermi energy) in a scattering calculation, where the spectrum is continuous, this choice may be limited in a calculation of the whole (discrete) spectrum of a finite network, or in a calculation which may involve several bands (or discrete energies) with gaps between them.

It is interesting to consider this comparison for a vertex on a linear chain, when $\mathcal{N}_\alpha = 2$. Even in this case, the parameters λ_α or ϵ_α would have to depend on energy, except for the trivial case $\lambda_\alpha = \epsilon_\alpha = 0$. The latter condition simply implies that this vertex is equivalent to any other point along the wire on which it "sits". Although appropriate in some cases, this cannot be generally valid. For example, this does not suffice to describe the configuration of two wires which meet at a finite angle.[17] Such a break in the straight line should cause scattering even if the wire itself is free of any scattering centers. To describe this scattering, one would need to introduce non-zero values for ϵ_α and/or λ_α. At this stage, we are not aware of a systematic study of this issue.

A priori, one might have thought that the two approaches should coincide when the lattice constant in the tight binding model approaches zero. Indeed, as noted above, the two models yield the same answers within each (uniform) linear chain. In the limit of vanishing a, Eq. (9) can be written as

$$(\epsilon + 2J)\psi_{\alpha\beta}(n) = -J[\psi_{\alpha\beta}(n-1) + \psi_{\alpha\beta}(n+1) - 2\psi_{\alpha\beta}(n)] \approx -Ja^2\frac{\partial^2\psi_{\alpha\beta}}{\partial x^2}\Big|_{x=na}. \quad (15)$$

This reproduces the continuum Schrödinger equation, provided we move the zero of energy to the bottom of the band, $-2J$, and identify the effective mass m via $\hbar^2/(2m) = Ja^2$, requiring that either $m \to \infty$ or $J \to \infty$ and $a \to 0$, such that Ja^2 is kept finite.

We next turn to the Schrödinger equation at the vertex, Eq. (12). In the limit of small a, we rewrite this equation as

$$(\epsilon - \epsilon_\alpha + \mathcal{N}_\alpha J)\Psi_\alpha = -J\sum_\beta [\psi_{\alpha\beta}(1) - \psi_{\alpha\beta}(0)] \approx -Ja\sum_\beta \frac{\partial\psi_{\alpha\beta}}{\partial x_{\alpha\beta}}\Big|_{x_{\alpha\beta}=0}. \quad (16)$$

For a finite effective mass m, $(\epsilon + 2J) \sim Ja^2k^2$ remains finite when $a \to 0$, and this equation becomes equivalent to Eq. (4) with

$$\lambda_\alpha \sim [\epsilon_\alpha - (\mathcal{N}_\alpha - 2)J]/(Ja). \quad (17)$$

In fact, this equation also follows from Eq. (14) in the limit of vanishing a. For $\mathcal{N}_\alpha \neq 2$, the two models coincide in this limit only if either $\lambda_\alpha \to \infty$ (i.e. the Dirichlet matching condition which implies $\Psi_\alpha = 0$) or $\epsilon_\alpha \sim (\mathcal{N}_\alpha - 2)J \sim 1/a^2 \to \infty$ i. e.

$$\epsilon_\alpha \approx (\mathcal{N}_\alpha - 2)J + \mu_\alpha/a, \quad a \to 0. \tag{18}$$

The correction term, μ_α, determines λ_α via $\lambda_\alpha = \mu_\alpha/(Ja^2)$. To reproduce the Kirchoff-Neumann-de Gennes matching conditions (2), one would need to have $\mu_\alpha = 0$.

At this stage, we have no direct information on how the tight binding Hamiltonian matrix elements vary with a for small a. In fact, the tight binding model was constructed to deal with small overlaps between the localized wave functions, which is no longer valid when $a \to 0$. However, it would still be interesting to have explicit microscopic mathematical calculations of the tight binding matrix elements, and to check whether indeed they all diverge as $1/a^2$. It would be even more interesting to find out whether the limiting tight binding matrix elements obey the relation (18).

An exception arises for a vertex on a linear chain, $\mathcal{N}_\alpha = 2$. In this case, Eq. (17) reduces to $\lambda_\alpha \sim \epsilon_\alpha/(Ja)$. For a finite effective mass on the wires, Ja^2 remains finite when $a \to 0$, and therefore $\lambda_\alpha \to 0$ whenever ϵ_α is finite, reproducing the Neumann matching condition.

Some of the papers which use tight binding models to describe mesoscopic systems actually use $\epsilon_n = 0$ for *all* the sites, except for a few resonant sites for which ϵ_n is varied by an external gate voltage. As explained, such a variation does not affect the Neumann matching conditions for $\mathcal{N}_\alpha = 2$ when $a \to 0$. However, if such gate voltages are applied to a vertex with more than two wires, then the parameter λ_α for that vertex will increase with decreasing a, crossing over to the Dirichlet condition and to the vanishing of the wave function on that vertex when $a \to 0$.

III. The T-shape scatterer

Quantum networks have been studied for a variety of geometries. Here we demonstrate the differences between the discrete tight binding and the continuum models on one of the simplest geometries. We calculate the transmission of an electron passing through a T-shaped device, consisting of a main wire attached to a stub of length L perpendicular to the wire at the origin $x = 0$ (Fig. 1).[13] Assuming that the electrons come from the left hand side, we expect a reflected wave on the left and a transmitted wave on the right hand side.

In the continuum approach, the wave function on the main wire is

$$\begin{aligned} \psi_w(x) &= e^{ikx} + re^{-ikx}, \quad && x \leq 0, \\ \psi_w(x) &= te^{ikx}, && x \geq 0, \end{aligned} \tag{19}$$

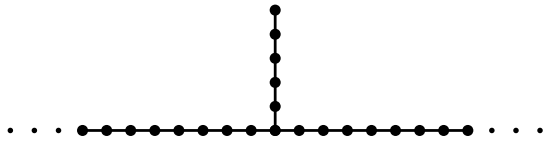

FIG. 1: A wire with a stub.

where r and t are the reflection and transmission amplitudes. Thus, $\psi_w(0) = 1 + r = t$. From Eq. (6), the wave function on the stub is given by

$$\psi_s(y) = \psi_w(0)\frac{\sin[k(L-y)]}{\sin(kL)}, \tag{20}$$

vanishing at $y = L$. Using Eq. (4) at the origin we find $t = 2/(2 + i[\cot(kL) + \lambda/k])$, and therefore the transmission through the main wire is

$$T = |t|^2 = 4/\big(4 + [\cot(kL) + \lambda/k]^2\big). \tag{21}$$

We note that this expression does not reproduce $T = 1$ for $L = 0$ and $\lambda = 0$, probably due to problems with the order of limits. For $L > 0$, T oscillates with k between 0 (full reflection) and 1 (full transmission). Sample results are shown in Fig. 2. Since $T(k) = T(-k)$, we show only results for $k > 0$. When $\lambda = 0$, $T(k)$ is periodic, with period π/L. However, for a non-zero energy-independent λ the transmission is no longer periodic, approaching the zero-λ behavior only for large k.

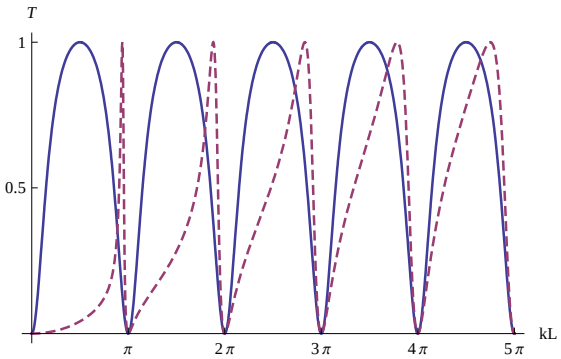

FIG. 2: Transmission for the continuum stub. The full (dashed) line represents $\lambda = 0$ ($\lambda = 3$).

We next consider the same model using the discrete equations. With a finite lattice constant a, the wave function is written as in Eq. (19), with x replaced by na. Similarly, we set $L = (N+1)a$ and replace y in Eq. (20) by ma, with $m = 0, 1, ..., N+1$, where N represents the number of bonds on the stub (5 in Fig. 1), after setting $\psi_s(N+1) = 0$. The tight binding equation at the origin then yields

$$t = 2/\big(2 + i\big[\cot[ka(N+1)] + \epsilon_0/[J\sin(ka)] - \cot(ka)\big]\big), \tag{22}$$

and $T = |t|^2$. It is easy to see the replacement given in Eq. (14). Note that (unlike Eq. (21), Eq. (22) does reproduce $T = 1$ for $N = 0$ and $\epsilon_0 = 0$.

Figure 3 compares the continuum result with $\lambda = 0$ (same as in Fig. 2) with the tight binding result with $\epsilon_0 = 0$, for $a = L/5$. As seen from Eq. (22), the transmission is now periodic with the new larger period π/a ($= 5\pi/L$ for the case drawn in Fig. 3). Therefore, we show only the lower half of the energy band, $0 < k < \pi/a$. As expected, the two models differ mostly near the edges of the energy band, where $\cot(ka)$ diverges. In contrast, the two approaches give very close results near the center of the band, $\epsilon \sim 0$ or $ka \sim \pi/2$. However, the difference between the two models increases as one moves away from this region.

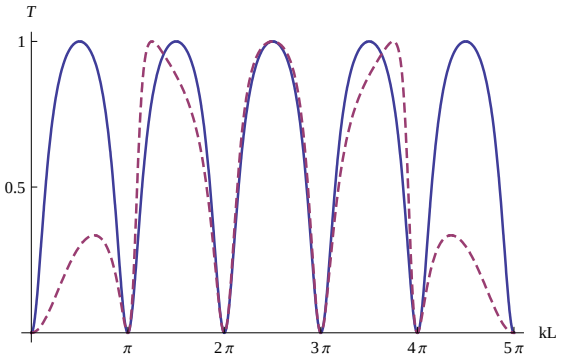

FIG. 3: Transmission for the continuum stub (full line), with $\lambda = 0$, and the tight binding stub (dashed line), with $\epsilon_0 = 0$, for $N + 1 = L/a = 5$.

The above results obviously change with the parameters λ and ϵ_0. For example, Fig. 4 compares the continuum model with $\lambda = 0$ with the tight binding model with $\epsilon_0/J = (\mathcal{N}_0 - 2) = 1$, for several values of a. As might be anticipated from Eq. (14), this value of ϵ_0 brings the tight binding equations close to the continuum ones near the bottom of the band, i. e. at small k. Indeed, Fig. 4 shows almost a coincidence of the results near $k = 0$. This coincidence improves as $N + 1 = L/a$ increases. However, the results are very different near the center of the band, $ka \sim \pi/2$.

IV. Conclusions

A detailed comparison between the tight binding "atomic" approach and the continuum approach to quantum networks reveals that the two models are generally different from each other, and one cannot expect them to yield the same results for all energies. However, the two models agree quantitatively near the center of the 1D band (which describes each of the wires in the network), $\epsilon \sim 0$. The two models are definitely very different near the band edges, where one encounters the van Hove singularities. Some of the differences between the models

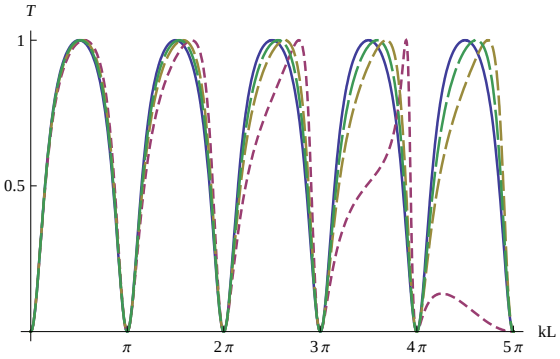

FIG. 4: Same as Fig. 3, but with $\epsilon_0/J = \mathcal{N}_0 - 2 = 1$. The dashed curves correspond to $N+1 = 5$, 10 and 20 (increasing dashes).

can be removed by adding appropriate site energies to the tight binding model, or by tuning the parameters of the matching conditions at the vertices of the continuous graphs. Sending the lattice constant to zero brings the two models close to each other near the bottom of the band only for very special choices of the site energies.

This paper presented only one simple example of a scattering solution, to demonstrate our main points. In such a scattering solution, where one is free to choose the energy of the scattered electrons near $\epsilon = 0$, the difference between the two approaches is small. This freedom does not exist in other situations. Foe example, we have recently followed Bercioux *et al.*[17,18] in considering an infinite chain of diamonds, where the electrons are subject to both the Aharonov-Bohm flux[28] and the Rashba spin-orbit interactions.[29] With these two effects, the various wave functions become 2-component spinors, and the basic hopping terms become 2×2 unitary matrices, which also contain phase factors. Furthermore, the probability current contains additional terms, due to these phases. Unlike Bercioux *et al.*, who found the spectrum of the diamond chain within the continuum model, we solved the same model within the tight binding approach, where each edge of each diamond represented a single bond.[27] We have since repeated this calculation with more "atoms" within each edge. Interestingly, the qualitative features of the resulting energy bands in the two approaches are similar. However, the interesting physics (e. g. the spin filtering found in Ref. 27) does involve moving away from the center of the basic 1D band. Therefore, the two approaches do yield different quantitative results. The continuum and the discrete approaches certainly give different results when one calculates the spectrum of a finite network. In this case, the resulting energies can assume any value, including values which are outside the "basic" band. In the latter case, the related k's are imaginary.

In the above discussion we have not attempted to judge which approach is "better". As we mentioned in passing, both approaches are sometimes oversimplified, miss-

ing some important physics. In practical situations, it is probably best to use both approaches and compare the results.

Acknowledgements. This paper is dedicated to the memory of Pierre Gilles de Gennes, with whom we had many illuminating discussions on many fields in physics. We acknowledge discussions and correspondence with Y. Imry, U. Smilansky and J. Vidal, and support from the ISF and from the DIP.

---

* Also emeritus, Tel Aviv University.
[1] Rudenberg, K.; Scherr, C. *J. Chem. Phys.* **1953**, 21, 1565.
[2] Griffith, J. S. *Trans. Faraday Soc.* **1953**, 49, 345.
[3] de Gennes, P. G. *C. R. S'eances Acad. Sci., Ser B* **1981**, 292, 9.
[4] de Gennes, P. G. *C. R. S'eances Acad. Sci., Ser B* **1981**, 292, 279.
[5] Alexander, S. *Phys. Rev. B* **1983**, 27, 1541.
[6] Büttiker, M.; Imry, Y.; Azbel, M. Ya. *Phys. Rev. A* **1984**, 30, 1982.
[7] Gefen, Y.; Imry, Y.; Azbel, M. Ya. *Phys. Rev. Lett.* **1984**, 52, 129.
[8] Büttiker, M. *Phys. Rev. B* **1985**, 32, 1846.
[9] Shapiro, B. *Phys. Rev. Lett.* **1983**, 50, 747.
[10] Kowal, D.; Sivan, U.; Entin-Wohlman, O.; Imry, Y. *Phys. Rev. B* **1990**, 42, 9009.
[11] Kottos, T.; Smilansky, U. *Phys. Rev. Lett.* **2000**, 85, 968.
[12] Xia, J.-B.; *Phys. Rev. B* **1992**, 45, 3593.
[13] Deo, P. S.; Jayannavar, A. M. *Phys. Rev. B* **1994**, 50, 11629.
[14] Kottos, T.; Smilansky, U. *Phys. Rev. Lett.* **1997**, 79, 4794.
[15] Akkermans, E.; Comtet, A.; Desbois, J.; Montambeaux, G.; Texier, C. *Ann. Phys.* **2000**, 284, 10.
[16] Vidal, J.; Montambeaux, G; Douçot, B. *Phys. Rev. B* **2000**, 62, R16294.
[17] Bercioux, D.; Governale, M.; Cataudella, V.; Ramaglia, V. M. *Phys. Rev. Lett.* **2004**, 93, 056802.
[18] Bercioux, D.; Governale, M.; Cataudella, V.; Ramaglia, V. M. *Phys. Rev. B* **2005**, 72, 075305.
[19] Avron, J. E.; Sadun, L. *Ann. Phys.* **1991**, 206, 440.
[20] Kottos, T.; Smilasky, U. *Ann. Phys.* **1999**, 274, 76.
[21] Texier, C.; Montambeaux, G. *J. Phys. A: Math. Gen.* **2001**, 34, 10307.
[22] Texier, C.; Büttiker, M. *Phys. Rev. B* **2003**, 67, 245410.
[23] Ashcroft, N. W.; Mermin, N. D. *Solid State Physics* **1976**, Saundes College,, Philadelphia, Ch. 10.
[24] Vidal, J.; Mosseri, R.; Douçot, B. *Phys. Rev. Lett.* **1998**, 81, 5888.
[25] Entin-Wohlman, O.; Aharony, A.; Imry, Y.; Levinson, Y; Schiller, A. *Phys. Rev. Lett.* **2002**, 88, 166801.
[26] Aharony, A.; Entin-Wohlman, O.; Halperin, B. I.; Imry, Y. *Phys. Rev. B* **2002**, 66, 115311.
[27] Aharony, A.; Entin-Wohlman, O.; Tokura, Y.; Katsumoto, S. *ArXiv* **2008**, 0805.3617.
[28] Aharonov, Y.; Bohm, D. *Phys. Rev.* **1959**, 115, 485.
[29] Rashba, E. I. *Fiz. Tverd. Tela (Leningrad)* **1960**, 2, 1224 [*Sov. Phys. Solid State* **1960**, 2, 1109].